Proceedings of the
44th IEEE Conference on Decision and Control, and
the European Control Conference 2005
Seville, Spain, December 12-15, 2005

Distributed delay model for density wave dynamics in gas lifted wells

Laure Sinègre*, Nicolas Petit
Centre Automatique et Systèmes
École des Mines de Paris
60, Bd Saint-Michel, 75272 PARIS Cedex
Email: sinegre,petit@cas.ensmp.fr
*corresponding author

Philippe Ménégatti
Centre Scientifique et Technique Jean Féger
TOTAL
Avenue Larribeau, 64000 PAU
Email: philippe.menegatti@total.com

Abstract— **Oil well instabilities cause production losses. One of these instabilities, referred to as the "density-wave" is an oscillatory phenomenon occurring on gas-lift artificially lifted well. We propose a distributed delay model of this dynamics. In order to interpret the observed oscillations we study the corresponding characteristic equation. Stabilization of this system is performed through a simple control law. Its performance is studied through realistic simulations.**

I. Introduction

Producing oil from deep reservoirs and lifting it through wells to surface facilities often requires activation to maintain oil output at a commercial level. In the gas-lift activation technique [3], gas is injected at the bottom of the well through the injection valve (point C in Figure 1) to lighten up the fluid column and to lower the gravity pressure losses. High pressure gas is injected at well head through the gas valve (point A in Figure 1), then goes down into the annular space between the drilling pipe (casing, point B) and the production pipe (tubing, point D) where it enters. Oil produced from the reservoir (point F) and injected gas mix in the tubing. They flow through the production valve E located at the surface.

As wells and reservoirs get older, liquid rates begin to decrease letting wells be more sensitive to flow instabilities commonly called headings. These induce important oil production losses (see [8]) along with possible facilities damages. Preventing instabilities through closed loop control has been an active field of research (see [10], [8] and [1]). These instabilities are defined as a flow regime characterized by regular and perhaps irregular cyclic changes in pressure at any point in the tubing string D (see [2]). Among these, one finds the "casing-heading" and the density-wave instability. "Casing heading" consists of a succession of pressure build-up phases in the casing without production and high flow rate phases due to intermittent gas injection rate from the casing to the tubing (see [10] for a complete description). The dynamics of the "casing heading" is well represented by a three balance ordinary differential equations model (proposed in [9], [6] and used in [12]). In the density-wave instability, which existence was first demonstrated in [8], oscillations are confined in the tubing D while the gas injection rate through valve C remains constant. Out-of-phase effects between the well influx and the total pressure drop along the tubing are usually reported at the birth of this phenomenon. In [8],

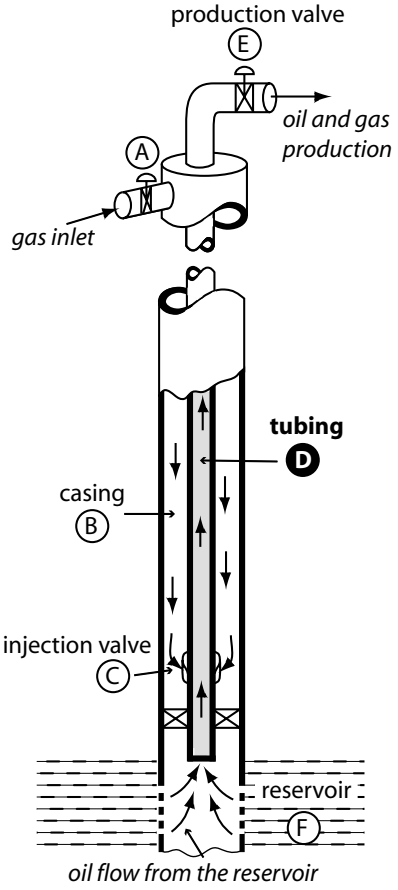

Fig. 1. Gas-lift activated well. Density-wave takes place in the tubing D.

dynamical choking is used to stabilise the density wave instability. In this paper, we propose a distributed delay model to represent and analyse the observed oscillations. Two applications of the model are presented: first a rigorous stability analysis demonstrating the impact of the gas flow rate and then an alternative control solution to [8] using the gas inlet A as an input and the downhole pressure measurements.

The paper is organized as follows. In Section II, we detail the observed oscillating phenomenon in gas-lift operations. In Section III, we derive a reference distributed delay model for the density propagation in the tubing. Main assumptions

0-7803-9568-9/05/$20.00 ©2005 IEEE

and the use of Riemann invariant are explicited along with boundary conditions. In Section IV, stability analysis of the corresponding characteristic equations is performed. Comparisons with OLGA®2000 are conducted and stress the role of the amount of injected gas. In Section V, we propose a control strategy relying on the model. Realistic simulations show that we can stabilize the flow.

II. Gas-lift operations

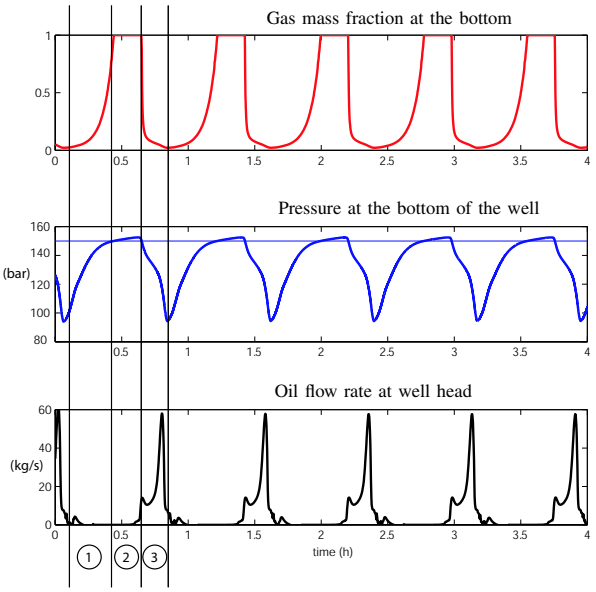

Fig. 2. Density wave simulated with OLGA®2000.

Figure 2 shows an example of density wave instability simulated with the transient multiphase flow simulator OLGA®2000. Typically, the depth of the well is 2500 m and the reservoir pressure is 150 bar. Oil production has an oscillating behavior consisting of 3 phases. In phase 1, there is no oil production at the surface but P_L, the pressure at the bottom of the well, is less than the reservoir pressure. Oil enters the pipe, letting P_L get closer to 150 bar. This is the self regulating mechanism of the well: the more is produced from the reservoir, the greater P_L becomes and eventually the less is produced. P_L is going to reach a constant which, in this case, is greater than 150 bar. The system switches to phase 2. This phase is characterized by zero oil production at the surface and from the reservoir (saturation of the oil flow rate at the bottom of the well). The gas mass fraction, which is close to 0 in phase 1, gets to a strictly positive constant in phase 2. Finally, the oil produced from the reservoir in phase 1 reaches the surface creating pressure drop in the well. This is phase 3. P_L decreases below 150 bar, oil flow rate at the bottom of the well increases and brings the fall of the gas mass fraction.

In summary, the density wave can be interpreted as the propagation of the mass fraction at the bottom of the well which is a result of a switching boundary condition.

Symb.	Constants	Values	Units
R	Gas perfect constant	287	S.I.
T	Temperature of the well	293	K
PI	Productivity Index	$4e-6$	kg/s/Pa
P_r	Reservoir pressure	$150e5$	Pa
P_0	Separator pressure	$10e5$	Pa
g	Gravity constant	9.81	m/s^2
ρ_l	Density of oil	800	kg/m^3
V^∞	Slip velocity constant	-	m/s
V_g	Gas velocity	0.8	m/s
β	Threshold parameter	0.03	
$u_{\min}$	Saturation value of u	0.1	bar
u_{ref}	Reference value of u	10	bar
$q_g^{\min}$	Saturation value of q_g	0.3	kg/s
L	Length of the pipe	2000	m

Symb.	Variables	Expressions	Units
$V_l(t,z)$	Oil velocity	$V_g + V^\infty/R_l$	m/s
$Rg(t,z)$	Gas volume fraction		
$R_l(t,z)$	Oil volume fraction	$R_g + R_l = 1$	
$x(t,z)$	Gas mass fraction		
$P(t,z)$	Pressure of the well		Pa
$x^L(t)$	Gas mass fraction at $z = L$		
$P_L(t)$	Pressure at $z = L$		Pa
$\rho_g(t,z)$	Gas density		kg/m^3
$\rho_m(t,z)$	Mixture density		kg/m^3
$q_l(t,z)$	Oil mass flux	$R_l\rho_l V_l$	kg/s/m^2
$q_g(t,z)$	Gas mass flux	$R_g\rho_g V_g$	kg/s/m^2
$u(t)$	Control $\simeq$ gas injection	$q_g/PI(1/\beta - 1)$	bar

TABLE I
NOMENCLATURE.

III. Proposed Model

We propose to study the density wave instability as a two phases flow problem in a vertical pipe filled with a mixture of oil and gas. The pressure at both ends are considered constant. Flows (gas and oil) enters the pipe at the bottom. The oil flow is given by the difference of pressure between the bottom of the pipe and the reservoir. The gas injection rate is considered constant (its value can be arbitrary updated for control purposes). Notations are given in Table I. Thanks to the choice of the slip velocity law (following [5]), we demonstrate the existence of a Riemann invariant. This lets the evolution of the distributed variables be summarized by the evolution of a single variable: the pressure at the bottom of the pipe.

A. Physics reduction

Pressure law: Using Bernoulli's law we get

$$P(t,z) = P_0 + \int_0^z \rho_m(t,\zeta) g d\zeta \tag{1}$$

Model (1) implies no friction term, it is consistent with the observed low flow rates for density wave instability (see [8]). Density of the mixture is given by

$$1/\rho_m = x/\rho_g + (1-x)/\rho_l$$

To work with a linear expression of ρ_m we assume that

$$\rho_m \sim x\rho_g + (1-x)\rho_l \tag{2}$$

Equivalently, we assume that the gas mass density is close to the gas volume density. Further, in the derivation of the

gas density, gas is considered perfect and the temperature T is constant. Besides we assume that the pressure gradient $\frac{P_r - P_0}{L}$ along the tubing is also constant and computed from boundary condition. Simulations have shown that this simplification improves the tractability while saving the oscillatory behavior. Using the expressions in (2) and after substitution in (1), we get

$$P(t,z) = P_0 + \rho_l g z + \int_0^z x(t,\zeta) g \left(\frac{(L-\zeta)P_0 + \zeta P_r}{LRT} - \rho_l \right) d\zeta \tag{3}$$

Slip velocity and Riemann invariant: We define the slip velocity (see [5]) as follows

$$V_g - V_l = \frac{V_\infty}{R_l}$$

Mass conservation laws write

$$\frac{\partial \rho_g R_g}{\partial t} + \frac{\partial q_g}{\partial z} = 0 \tag{4}$$

$$\frac{\partial \rho_l R_l}{\partial t} + \frac{\partial q_l}{\partial z} = 0 \tag{5}$$

As

$$x = \frac{R_g \rho_g}{R_g \rho_g + R_l \rho_l} \tag{6}$$

one can combine (4), (5) and (6), to obtain

$$\frac{\partial x}{\partial t} + V_g \frac{\partial x}{\partial z} = 0$$

meaning that x is a Riemann invariant (see [4]). For sake of simplicity we assume V_g to be constant. On real wells it is not as simple and we shall discuss the implications of this hypothesis in Section V-C. This implies

$$x(t,z) = x\left(t - \frac{L-z}{V_g}, L\right) = x^L\left(t - \frac{L-z}{V_g}\right)$$

Therefore, knowing bottom well gas mass fraction $t \mapsto x^L(t)$, we get the profile $(t,z) \mapsto x(t,z)$ in the tubing. Replacing this expression in equation (3) and denoting $P_L(t) = P(t,L)$, we find

$$P_L(t) = P_L^\star + \int_{t-\delta}^{t} k(t-\tau) x^L(\tau) d\tau \tag{7}$$

with

$$\delta = L/V_g \tag{8}$$

$$P_L^\star = P_0 + \rho_l g L \tag{9}$$

and

$$[0,\delta] \ni t \mapsto k(t) \triangleq V_g g \left(\frac{tP_0 + (\delta - t)P_r}{\delta RT} - \rho_l \right) < 0 \tag{10}$$

Notice that k is a strictly decreasing affine function.

Boundary condition: Classically, (see [3]), the oil rate q_l is given at the reservoir boundary by the Productivity Index (PI) through

$$q_l(t,L) = PI \max(P_r - P_L(t), 0) \tag{11}$$

By definition,

$$x^L(t) = \frac{1}{1 + PI/q_g \max(P_r - P_L(t), 0)} \tag{12}$$

We want to simplify this last expression in the case of large PI. On one hand, as $P_r - P_L$ begins to be positive, x^L goes to zero. Let β denote a threshold parameter. In particular $x^L < \beta$ is equivalent to $P_L < P_r - \frac{q_g}{IP}(1/\beta - 1)$. We denote

$$u \triangleq q_g \frac{1}{PI}(1/\beta - 1) \tag{13}$$

On the other hand, when $P_L > P_r$, $x^L = 1$. Therefore, we consider x^L as constant, equal to 1 when $P_L > P_r$ and equal to 0 when $P_L < P_r - u$. Finally, the considered expression of x^L reduces to

$$x^L = h\left(X\right),\ X \triangleq 1 - \frac{P_r - P_L}{u} \tag{14}$$

with

$$h(\cdot) = \max(\min(1, \cdot), 0)$$

Equation (14) is the definition we use instead of Equation (12) from now on.

B. Density-wave as a distributed delay model

We now gather equations (7) and (14), and consider an initial condition $[-\delta, 0] \ni t \mapsto \phi(t) \in \mathbb{R}$. The following model represents the density wave phenomenon by the evolution of the pressure at the bottom of the well P_L

$$\begin{cases} P_L(t) = P_L^\star + \displaystyle\int_{t-\delta}^{t} k(t-\tau) h\left(1 - \frac{P_r - P_L(\tau)}{u(\tau)}\right) d\tau \\ P_L(t) = \phi(t),\ t \in [-\delta, 0] \end{cases} \tag{15}$$

where δ is the transport delay defined in (8), $P_L^\star$, given in (9), is the pressure at the bottom of the pipe when it is full of oil and P_r is the pressure of the reservoir. k is an affine function, given in (10). It depends on the considered fluids. u is proportional to q_g (see equation (13)). It can be arbitrarily updated and thus can be considered as a control.

C. Simulation results

Figure 3 shows the simulations results of (15). When $P_r = 150$ bar and $u = 10$ bar, we get an oscillating trajectory which presents similarities with Figure 2. Indeed, the periodic behavior consist of 3 phases. Alternatively, out of phase switches of $h(X(t))$ and $h(X(t-\delta))$ result in 4 slope changes of P_L. These reproduce the 3 phases observed in Figure 2: oil production from the reservoir (1), followed by pressure buildup (2), and eventual pressure drop (3).

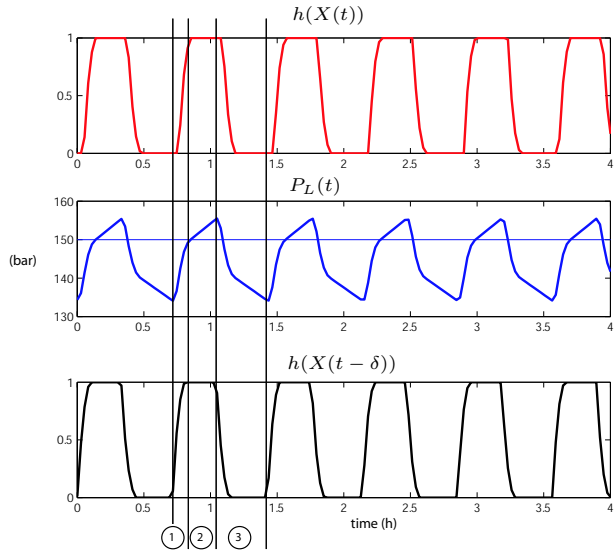

Fig. 3. Density wave simulated with equation (15) in Matlab. The reservoir pressure P_r is 150 bar and u is set at 10 bar.

D. Reference model for stability analysis

Model (15) will be used in Section V-A to design the control law for u. To study stability it is equivalent (but more convenient) to consider X as defined in equation (14). It follows from (15)

$$X(t) = 1 - \frac{P_r - P_L^\star}{u} + \frac{1}{u}\int_{t-\delta}^{t} k(t-\tau)h(X(\tau))d\tau \quad (16)$$

By derivation (assuming u constant), we get

$$u\dot{X}(t) = k(0)h(X(t)) - k(\delta)h(X(t-\delta)) + k'(0)\int_{t-\delta}^{t} h(X(\tau))d\tau \quad (17)$$

We consider the system (17) with initial condition ϕ defined and continuous on $[-\delta, 0]$, satisfying:

$$\phi(0) = 1 - \frac{P_r - P_L^\star}{u} + \frac{1}{u}\int_{0-\delta}^{0} k(t-\tau)h(\phi(\tau))d\tau$$

For this class of initial conditions, equations (16) and (17) have the same solutions.

IV. Stability

We first study the stability of the trivial solution of the following saturation-free model derived from equation (17). We denote

$$\tau \triangleq \delta/u \quad (18)$$

and $\mathcal{C}$ the (Banach) space of continuous function mapping the interval $[-\tau, 0]$ into $\mathbb{R}$. We define $x_t \in \mathcal{C}$ as

$$[-\tau, 0] \ni \theta \mapsto x_t(\theta) = x(t+\theta)$$

By derivation and time scaling, equations (17) rewrites

$$\begin{cases} \dot{x}(t) = f(x_t) \text{ for } t \geq 0 \\ x(t) = \phi(t) \text{ for } t \in [-\tau, 0] \end{cases} \quad (19)$$

with $\phi \in \mathcal{C}$ and $f : \mathcal{C} \to \mathbb{R}$ defined as,

$$f(x_t) = ax(t) + bx(t-\tau) + \frac{c}{\tau}\int_{t-\tau}^{t} x(\zeta)d\zeta \quad (20)$$

with $a + b + c = 0$, $b > 0$, $c < 0$ and $b + c > 0$ (by equation (10)). Referring to the formulation used in [7], one can rewrite equation (19) as

$$f(x_t) = \int_{-\tau}^{0} d(\eta(\theta))x_t(\theta) \quad (21)$$

With

$$\begin{cases} \eta(\theta) = (c/\tau)\theta, \quad \theta \in]-\tau, 0[\\ \eta(0) = a \\ \eta(-\tau) = -(c+b) \end{cases}$$

As η is continuous on $]-\tau, 0[$ and has bounded variation on $[-\tau, 0]$, given any $\phi \in \mathcal{C}$, there exists a unique function x_t, continuous, that satisfies system (19). We now study stability of (19) through the solutions of its characteristic equation. As will appear, stability depends on τ.

A. Characteristics equation solutions

The characteristic equation associated with (19) writes

$$s = a + be^{-s\tau} + \frac{c}{s\tau}(1 - e^{-s\tau}) \quad (22)$$

This equation is well defined by continuity at 0 and for all $\tau \geq 0$, 0 is an isolated solution. Referring to the necessary condition expressed in [13], as, for all $\tau \geq 0$

$$\det(\eta(-\tau) - \eta(0)) = -(a+b+c) = 0 \leq 0,$$

the trivial solution is not asymptotically stable.

In the following, we characterize the location of the non zero roots with respect to τ. In Proposition 1, we exhibit a family $(\tau_k)_{k\in\mathbb{N}}$ at which two roots hit the imaginary axis. Then we show that, for small τ, roots are lying on the left half plane (Proposition 2). Further, proving that the roots cross the imaginary axis from left to right, we conclude towards the existence of $\tau^\star > 0$ (Proposition 3) such that

- for $\tau \in [0, \tau^\star[$, all roots except 0 have strictly negative real part
- for $\tau > \tau^\star$, there is at least one root with strictly positive real part.

Proposition 1. *Consider the following system*

$$\dot{x}(t) = ax(t) + bx(t-\tau) + \frac{c}{\tau}\int_{t-\tau}^{t} x(\zeta)d\zeta \quad (23)$$

with $a + b + c = 0$, $b > 0$, $c < 0$, $b + c > 0$ and $\tau > 0$. Let $\lambda = c/b$. There exists $(\tau_k, \omega_k)_{k\in\mathbb{N}} \in \mathbb{R}^+ \times \mathbb{R}^+$ such that, for $\tau = \tau_k$, besides 0 which is always a solution, the pure imaginary roots of the characteristic equation of (23) are $\pm j\omega_k$. This family (τ_k, ω_k) is defined by

$$\begin{cases} \cos(\omega_k\tau_k) = 1 + \dfrac{\lambda\sigma_k}{\sigma_k - (2+\lambda)} \\ \omega_k \sin(\omega_k\tau_k) = \dfrac{c\sigma_k(2+\lambda)}{\sigma_k - (2+\lambda)} \\ \omega_k^2 = b^2(2+\lambda)^2\left(\dfrac{-\lambda}{2+\lambda}\dfrac{\sigma_k}{\sigma_k - 2}\right) \end{cases} \quad (24)$$

with $\sigma_k = (2b+c)\tau_k + 2 > 3 + \lambda$.

Proof: We are now looking for pure imaginary roots of equation (22). If there exists $\tau \geq 0$ such that $j\omega$ is solution then $-j\omega$ is also a solution. Therefore, we restrict our study to $(\tau, \omega) \in \mathbb{R}^+ \times \mathbb{R}^+ \backslash \{0\}$. Equation (22) yields

$$\begin{cases} b\cos(\omega\tau) + \dfrac{c}{\tau\omega}\sin(\omega\tau) = b + c \\ \dfrac{c}{\tau\omega}\cos(\omega\tau) - b\sin(\omega\tau) = \omega + \dfrac{c}{\tau\omega} \end{cases} \tag{25}$$

This implies

$$\omega^2 = -\frac{c}{\tau}\left(2b\tau + c\tau + 2\right) \tag{26}$$

By construction, $\lambda \in]-1, 0[$. Note $\sigma = (2b+c)\tau + 2 \geq 0$. Equation (25) leads to

$$\cos(\sqrt{-\frac{\lambda}{2+\lambda}\sigma(\sigma-2)}) = 1 + \frac{\lambda\sigma}{(\sigma-2)-\lambda} \tag{27}$$

$$\sin(\sqrt{-\frac{\lambda}{2+\lambda}\sigma(\sigma-2)}) = \frac{1}{\omega}\frac{c\sigma(2+\lambda)}{\sigma-2-\tau} < 0 \tag{28}$$

We derive from inequality (28) that $\sigma \in \bigcup_{k\in\mathbb{N}}\left[1+\sqrt{1+\frac{2+\lambda}{-\lambda}(2k+1)^2\pi^2}, 1+\sqrt{1+\frac{2+\lambda}{-\lambda}4k^2\pi^2}\right]$. Right hand side of equation (27) approaches $0 < 1+\lambda < 1$ as σ goes to infinity. The left hand side is oscillating thanks to the cos function and equation (27) has an infinite number of solutions. Among these, we keep those compatible with equation (28) and gather them in $(\sigma_i)_{i\in\mathbb{N}}$, an increasing sequence. By construction,

$$\lim_{i\to\infty}\sigma_i = +\infty$$

and

$$\sigma_i \sim_{i+\infty} \sqrt{\frac{2+\lambda}{-\lambda}}2i\pi$$

Further, for all $k \in \mathbb{N}$

$$1+\sqrt{1+\frac{2+\lambda}{-\lambda}(2k+1)^2\pi^2} > 1+\sqrt{1+\pi^2} > 3+\lambda$$

The set $(\sigma_i)_{i\in\mathbb{N}}$ is thus bounded by below

$$\forall k \in \mathbb{N}, \quad \sigma_k > 3 + \lambda \tag{29}$$

This set defines a family of solutions of equation (25), $(\tau_k, \omega_k)_{k\in\mathbb{N}}$ using equation (26)

$$\tau_k = \frac{\sigma_k - 2}{2b+c}$$
$$\omega_k^2 = b^2(2+\lambda)^2\left(\frac{-\lambda}{2+\lambda}\frac{\sigma_k}{\sigma_k-2}\right)$$

■

Lemma 1. *Define s a non zero root of the characteristic equation* (22)*. For all $\alpha > -1$, $\beta > 0$ and $\tau_\alpha > 0$ there exists $\tau \leq \tau_\alpha$ such that:*

$$|s(\tau)| > \beta\tau^\alpha$$

Proof: Assume that one can find $(\alpha, \tau_\alpha, \beta)$ ($\alpha > -1$, $\beta > 0$ and $\tau_\alpha > 0$) such that for all $\tau \leq \tau_\alpha$

$$|s| \leq \beta\tau^\alpha$$

Thus $|s\tau| \to 0$ as $\tau \to 0$. A second order development of (22) yields

$$\frac{1}{\tau} = -b - \frac{c}{2} + \left(\frac{b}{2} + \frac{c}{6}\right)s\tau + o(s\tau)$$

The right hand side of this development goes to $-b - c/2$ as $\tau \to 0$ and the left hand side to $+\infty$. This cannot be, therefore, the assumption is false. ■

Lemma 2. *Define s a non zero root of the characteristic equation* (22)*. For all τ_r, there exists $\tau \leq \tau_r$ such that*

$$\boldsymbol{Re}(s(\tau)) < 0$$

Proof: Assume that there exists τ_r such that for all $\tau \leq \tau_r$

$$\mathbf{Re}(s(\tau)) \geq 0$$

It follows that $|e^{-s\tau}| \leq 1$ and that $|\frac{1-e^{-s\tau}}{s\tau}| \leq 1$. Using Equation (22) we get

$$|s(\tau)| \leq |a| + |b| + |c|$$

which is in contradiction with Lemma 1. ■

Proposition 2. *There exists $\underline{\tau} > 0$ such that for all $\tau \leq \underline{\tau}$ the roots of the characteristic equation* (22) *that are not zero are strictly lying on the left half plane.*

Proof: Consider a non zero root. From Proposition 1, we know that, for $\tau < \tau_1$, it does not intersect the imaginary axis. Further, we know, from Lemma 2, that there exists $\tau < \tau_1$ such that the root lies on the left half plane. As the real part of the root is continuous with respect to τ (by the implicit function theorem), the root cannot go to the right part without crossing the imaginary axis. This implies that, for all $\tau < \tau_1$ the root is in the left half plane. Finally, for all $\tau \in [0, \tau_1[$, all roots except 0 have strictly negative real part. This concludes the proof. ■

Proposition 3. *There exists τ^* such that for all $\tau \in [0, \tau^*[$ the characteristic equation* (22) *has one root at* 0 *and all other roots strictly in the left part of the complex plane. For all $\tau > \tau^*$ there exists at least one root lying strictly on the right half plane.*

Proof: Let τ be positive. As proven in Proposition 2, for small τ all roots except 0 lie in the left half plane. To know whether these roots become unstable or come back to the left hand side, we compute $\mathbf{Re}\frac{\partial s}{\partial\tau}_{|\pm j\omega_k}$. We use equations (24) and after some computations we get

$$\frac{\partial s}{\partial\tau}_{|s=j\omega} = \frac{-b\omega^2 e^{-j\omega\tau} + \frac{c}{\tau^2}(1-e^{-j\omega\tau}) - \frac{cj\omega}{\tau}e^{-j\omega\tau}}{-2j\omega - b - c + be^{-j\omega\tau} - bj\omega\tau e^{-j\omega\tau} + ce^{-j\omega\tau}}$$

and

$$\mathbf{Re}\frac{\partial s}{\partial \tau}_{|\pm j\omega_k} = -\frac{\lambda b^2(2+\lambda)^3(\sigma_k-3-\lambda)}{(\sigma_k^2+(2\lambda^2-2+5\lambda)\sigma_k-2\lambda(3+\lambda)^2)(u_k-2)}$$

From (29) and noticing that $\sigma_k^2+(2\lambda^2-2+5\lambda)\sigma_k-2\lambda(3+\lambda)^2>0$ for $\sigma_k>2$, we have

$$\mathbf{Re}\frac{\partial s}{\partial \tau}_{|\pm j\omega_k} > 0$$

Therefore, after crossing the imaginary axis the roots always go to the right half plane. Thus simply, $\tau^* = \tau_1 = \frac{\sigma_1-2}{2b+c}$. ■

B. Conclusion

Parameter τ has a direct impact on the roots location of the characteristic equation. Increasing the time delay τ or letting the roots be unstable are equivalent. Recalling $\tau = \frac{\delta}{u}$, this last remark means that there exists a minimal gas injection rate that guarantees stability of the roots. Study of the characteristic equation is a key to the interpretation of the observed oscillating behavior. Depending on u trajectories of model (17) behave as follows. Unstable solutions of the model (17), which, initially match with unstable solutions of a linear system of type (20), finally reach saturation yielding behaviors depicted in Figure 3. Stable solutions remain bounded and if the initial condition is well chosen (e.g. constant) they do not reach the saturation.

V. Control

In this section, we design control laws to steer system (15) to a predefined steady state.

A. Control laws definition

We look for control laws u such that P_L converges to a chosen constant $P_{\text{ref}} \in \left]P_L^\star + \int_0^\delta k(\tau)d\tau, P_L^\star\right[$. The corresponding steady state value of X defined in (14) is

$$X_{\text{ref}} = -\frac{P_L^\star - P_{\text{ref}}}{\int_0^\delta k(\tau)d\tau} \in]0,1[\tag{30}$$

We note u_{ref} the value of u at steady state. It satisfies

$$X_{\text{ref}}(u_{\text{ref}}) = \frac{P_L^\star - P_r + u_{\text{ref}}}{u_{\text{ref}} - \int_0^\delta k(\tau)d\tau} \tag{31}$$

Our (closed-loop) control law is, simply,

$$u(t) = \frac{P_r - P_L(t)}{1 - X_{\text{ref}}} \tag{32}$$

This control strategy feeds system (15), which has finite memory δ, with a constant term. By direct computation, this straightforward approach provides convergence. We can state the following proposition.

Proposition 4. *With control law* (32)*, P_L which dynamics is defined by system* (15) *converges to P_{ref} in finite time δ for any initial condition $[-\delta, 0] \ni t \mapsto \phi(t) \in \mathbb{R}$.*

Yet, the expression u defined in (32) does not take into account actuation saturations. Here, the most limiting factor in practice is a lower bound $u_{\min} > 0$ on the control. It is often reached with this naive approach. We now propose the saturated control law

$$\begin{cases} u = \dfrac{P_r - P_L(t)}{1 - X_{\text{ref}}}, \text{ for } P_L < P_r - u_{\min}(1 - X_{\text{ref}}) \\ u = u_{\min}, \text{ for } P_L \geq P_r - u_{\min}(1 - X_{\text{ref}}) \end{cases} \tag{33}$$

Proposition 5. *Assume that*

$$X_{ref} \geq \frac{P_L^\star - P_r + u_{min}}{u_{min} - \int_0^\delta k(\tau)d\tau} \tag{34}$$

With the (saturated) control law (33)*, P_L which dynamics is defined by system* (15)*, converges to P_{ref} in finite time 2δ for any initial condition $[-\delta, 0] \ni t \mapsto \phi(t) \in \mathbb{R}$.*

Proof: We now show that for $t \geq \delta$, the control law is unsaturated. Indeed, for $t > 0$

$$h\left(1 - \frac{P_r - P_L(t)}{u(t)}\right) \geq X_{\text{ref}}$$

Therefore, for all $t \in [\delta, +\infty[$,

$$P_L(t) \leq P_L^\star + X_{\text{ref}} \int_0^\delta k(\tau)d\tau$$

Assuming (34), a simple computation yields

$$\forall t \geq \delta,\ P_L(t) \leq P_r - u_{\min}(1 - X_{\text{ref}})$$

By equation (33), we get that, for all $t \geq \delta$, u is simply defined by

$$u = \frac{P_r - P_L(t)}{1 - X_{\text{ref}}}$$

The control is thus unsaturated and, by Proposition 4, we conclude that system (15) converges towards P_{ref} in 2δ. ■

In practice, one must choose P_{ref} in accordance to the minimum value $u_{\min}$ such that equation (31) holds. This choice implies that assumption (34) holds.

Indeed, if $P_r > P_L^\star + \int_0^\delta k(\tau)d\tau$, which simply means that the pressure at the bottom of pipe when it is full of gas is smaller than the reservoir pressure, then $u_{\text{ref}} \mapsto X_{\text{ref}}(u_{\text{ref}})$, given in (31), is increasing. Therefore, if $u > u_{\min}$

$$X > \frac{P_L^\star - P_r + u_{\min}}{u_{\min} - \int_0^\delta k(\tau)d\tau}$$

The meaning of assumption (34) is that one should not define P_{ref} outside the range of X that can be reached with $u > u_{\min}$.

B. Simulation

Figure 4 shows an example of stabilization with the saturated control law (33). Choosing $u = 10$ bar and using equations (30) and (31) we compute the corresponding steady states $P_{\text{ref}} = 145$ bar and $X_{\text{ref}} = 0.464$. We define $u_{\min} = 0.1$, which satisfies assumption (34). Until t_c the system is left open loop. At $t = t_c$, the controller is turned on. From t_c to $t_c + \delta$, the gas mass fraction $h(X(t))$ remains between X_{ref} and 1. Therefore, for $t > t_c + \delta$, $P_l(t)$ remains below $P_{\max} = P_r - u_{\min}(1 - X_{\text{ref}}) = 150$ bar and $h(X(t)) = X_{\text{ref}}$. Pressure P_L converges to P_{ref} in finite time.

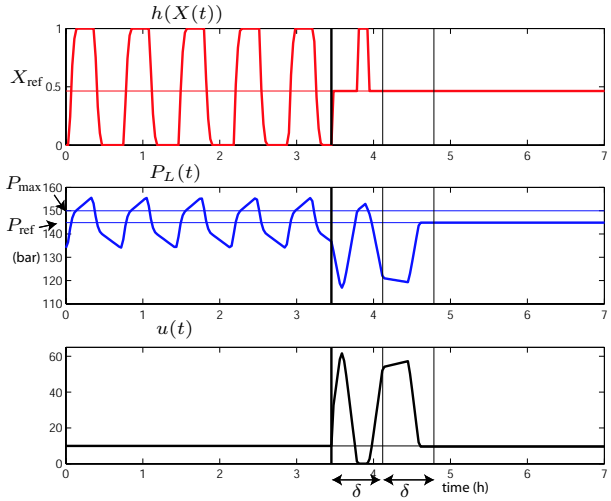

Fig. 4. Stabilization of equation (15) using the saturated control law (33). Control is switched on after approximatively 3.4 hours of open loop. P_L reaches P_{ref} and X reaches X_{ref} in finite time 2δ.

An alternative view is given in Figure 5. Left three snapshots describe the open-loop behavior. Gas mass fraction profile, $x(t,z)$, is represented in white (complementary black part stands for oil mass fraction). Boundary condition q_g is constant and q_l is defined by equation (11). Finally, the right scheme represents the transient obtained with closed loop control. The feeds keep the gas mass ratio constant at X_{ref}. During the transient, q_g is permanently adapted to counteract the effect of the state $x(t,z)$, $z \in [0,L]$, onto q_l. This yields a constant $X(t,L)$ which progressively steers the system to steady state through the transport equation.

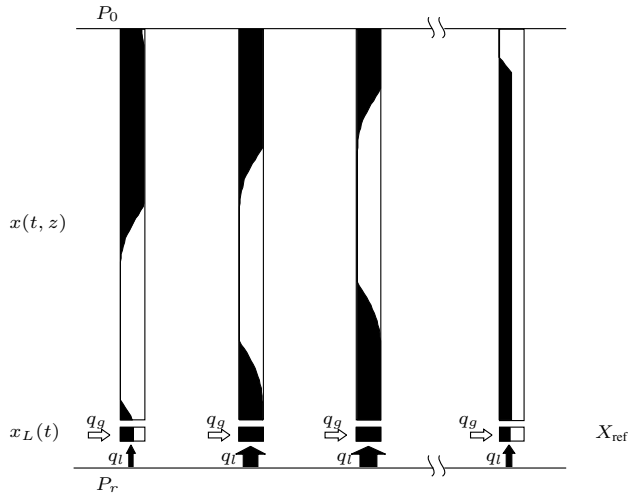

Fig. 5. Comparison of open loop (3 schemes on the left) and closed loop behavior.

C. Stabilization of the well simulated in OLGA®2000

The closed loop control law can be tested in OLGA®2000 Transient Multiphase Flow Simulator. A realistic dynamic oil-gas model is used along with semi-implicit numerical solver (see [11] for details).

In Section III-A, we assume the gas velocity to be constant, i.e. we neglect the impact of the gas mass fraction on the gas velocity. Therefore, when the gas mass flow rate is high enough, this assumption only results in a time depending time dilatation. But when the gas inlet is too low the well production eventually stops, which is not represented by the simple model. Therefore we want the gas injection rate to remain above a minimum, $q_g^{\min}$, guaranteeing the flow in the pipe. This defines a lower bound for our control law. Following the same lines as in the previous section, we define the control q_g, corresponding to u (see equation (13)), to keep x^L at a predefined constant, X_{ref}. Using x^L given in equation (12), our control law writes

$$q_g(t) = \max\left(\frac{X_{ref}}{1-X_{ref}} IP(P_r - P_L(t)), q_g^{\min}\right)$$

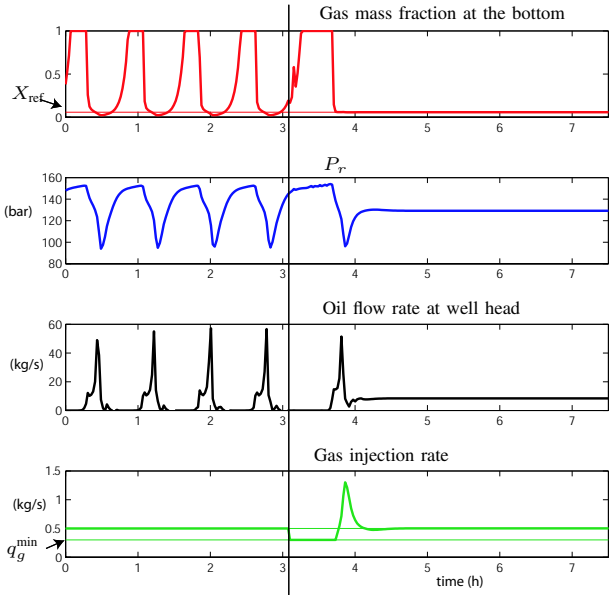

Fig. 6. Stabilization of density wave instability simulated in OLGA®2000. $X_{\text{ref}} = 0.0568$ and $q_g^{\min} = 0.3$.

Figure 6 shows an example of stabilization of density wave instability. We define $q_g^{\min} = 0.3$ kg/s and $X_{\text{ref}} = 0.0568$. The controller is switched on at the black line and steers the well to the steady state corresponding to the initial gas injection rate. As the period of the oscillations corresponds approximately to the travel time δ, we see in Figure 6 that the well is stabilized in 2δ. As shown in Proposition 5, 2δ corresponds to the time needed by the well to forget its initial condition.

VI. Conclusion

In this paper we propose an interpretation of the observed oscillations in the tubing of gas lifted wells. A distributed parameter model has been derived for the propagation of pressure (system (15)). It describes the dynamics as a transport phenomenon with state dependent boundary condition.

This equation is shown to be equivalent to a saturated linear delay model (equation (17)) involving the gas fraction. Analysis of the underlying characteristic equation is performed (for unsaturated solutions) and show that the critical parameter is the amount of injected gas. This is consistent with state-of-the-art and suggests a simple control strategy. Performance of the derived control strategy is demonstrated through OLGA® 2000 simulations, proving that it is possible to obtain a steady flow with the same amount of injected gas, after a finite time transient during which the oscillation is cancelled. The main restriction of this strategy is that downhole measurements are often not available. Therefore we are investigating a way to maintain the gas mass fraction constant at the entrance of the tubing using only topside measurements.

Acknowledgements: The authors are indebted to Emmanuel Duret and Pierre Rouchon for insightful discussions.

REFERENCES

[1] O. M. Aamo, G. O. Eikrem, H. Siahaan, and B. Foss, "Observer design for multiphase flow in vertical pipes with gas-lift - theory and experiments," *Journal of Process Control*, vol. 15, pp. 247–257, 2005.

[2] E. P. Blick, P. N. Enga, and P. C. Lin, "Theoretical stability analysis of flowing oil wells and gas-lift wells," *SPEPE*, pp. 508–514, 1988.

[3] K. E. Brown, *Gas lift theory and practice*. Petroleum publishing CO., Tulsa, Oklahoma, 1973.

[4] A. J. Chorin and J. E. Marsden, *A mathematical introduction to fluid mechanics*. Springer-Verlag, 1990.

[5] E. Duret, "Dynamique et contrôle des écoulements polyphasiques," Ph.D. dissertation, École des Mines de Paris, 2005.

[6] G. O. Eikrem, L. Imsland, and B. Foss, "Stabilization of gas-lifted wells based on state estimation," in *Proc. of the 2nd IFAC Symposium on System, Structure and Control*, 2004.

[7] J. K. Hale and S. M. V. Lunel, *Introduction to functional differential equations*. Springer-Verlag, 1993.

[8] B. Hu and M. Golan, "Gas-lift instability resulted production loss and its remedy by feedback control: dynamical simulation results," in *SPE International Improved Oil Recovery Conference in Asia Pacific*, no. SPE 84917, Kuala Lumpur, Malaysia, 2003.

[9] L. S. Imsland, "Topics in nonlinear control - ouput feedback stabilization and control of positive systems," Ph.D. dissertation, Norwegian University of Science and Technology, Department of Engineering and Cybernetics, 2002.

[10] B. Jansen, M. Dalsmo, K. Havre, L. Nøkleberg, V. Kritiansen, and P. Lemétayer, "Automatic control of unstable gas-lifted wells," *SPE Annual technical Confererence and Exhibition.*, no. SPE 56832, October 1999.

[11] Scandpower, *OLGA® 2000 User's Manual*. Scandpower, 2004.

[12] L. Sinègre, N. Petit, P. Lemétayer, P. Gervaud, and P. Ménégatti, "Casing heading phenomenon in gas lifted well as a limit cycle of a 2d model with switches," in *Proc. of the 16th IFAC World Congress*, 2005.

[13] G. Stépán, *Retarded dynamical systems: stability and characteristic functions*, ser. Pitman Research Notes in Math. Series. UK: Longman Scientific, 1989.